

# Universal Electroluminescence at Voltages below the Energy Gap in Organic Light-Emitting Diodes

Yungui Li,\* Oskar Sachnik, Bas van der Zee, Kalyani Thakur, Charusheela Ramanan, Gert-Jan A. H. Wetzelaer,\* and Paul W. M. Blom\*

In organic light-emitting diodes (OLEDs), it is typically assumed that a voltage equal to or higher than the energy gap of the emitters is required to observe electroluminescence (EL). However, EL at subgap voltages is observed and proposed to originate from up-conversion processes, such as fusion of low-energy triplet excitons. Here, it is demonstrated that EL at subgap voltages in OLEDs is universally present. By using emitters with negligible energy splitting between the singlet and triplet state, the need for incorporating low-energy triplet excitons is ruled out. The origin of EL at voltages below the energy gap is the recombination of diffused and thermally generated charge carriers, universally present in light-emitting diodes at nonzero temperatures, theoretically permitting electrical-to-optical power-conversion efficiencies exceeding unity.

annihilation (TTA) to form an emitting singlet<sup>[1,6–8]</sup> and band-to-band recombination.<sup>[9,10]</sup> EL has even been observed in devices without such heterojunction, for which it was proposed that electrons could be injected directly into a low-energy triplet state, followed by emissive singlet exciton formation via triplet fusion.<sup>[7]</sup> However, it should be noted that EL at subgap voltages has been widely observed in diodes based on inorganic semiconductors, in which processes such as TTA likely do not play a role.<sup>[11–14]</sup>

Here, we demonstrate that EL at subgap voltages is a universal feature of OLEDs. Even down to zero applied voltage, EL is theoretically present, which is the result of

the recombination of diffused and thermally generated charge carriers. Consequently, for an ideal OLED without traps and Ohmic contacts, the electrical quantum efficiency (EQE,  $\Gamma_{\text{EL}}$ ) for EL equals unity down to zero applied voltage. Experimentally, EL at voltages below the energy gap is clearly observed in OLEDs based on emitters with negligible energy difference between the singlet and triplet excited states, ruling out energy up-conversion mediated by low-energy triplet states. Furthermore, also in OLEDs with a strongly reduced free carrier density due to trapping the EL at subgap voltages occurs, ruling out Auger processes that require high carrier densities.

## 1. Introduction

In organic light-emitting diodes (OLEDs), the minimum operating voltage at which electroluminescence (EL) is observed is typically larger than the optical energy gap divided by the elementary charge,  $E_g/q$ . This is commonly rationalized by the idea that an electron requires an electrical energy input at least equal to the energy of the emitted photon in order not to violate the energy conservation law. On the contrary, OLEDs have been reported exhibiting EL at voltages well below the energy gap of the emitter.<sup>[1–3]</sup> Typically, such devices involve a heterojunction with large energy offsets, e.g., the commonly studied heterojunction devices based on rubrene and C<sub>60</sub>. However, the origin of the low-voltage EL is debated. Three different mechanisms have been proposed, including Auger recombination at the heterojunction interface,<sup>[4,5]</sup> the formation of triplet excitons via the interfacial charge-transfer state, followed by triplet–triplet

## 2. Results and Discussion

Consider a simple OLED in which an emitting semiconductor layer is sandwiched between Ohmic electron- and hole-injecting contacts, for which the energy band diagram is displayed in **Figure 1a**. At zero applied voltage, a built-in electric field exists that points toward the collect contacts, due to the asymmetry of the electrode work functions. By applying a small voltage, a diffusion current in the opposite direction of the electric field starts to flow, depending exponentially on the applied voltage (see Equation (1)). When the applied voltage reaches the built-in voltage, determined by the difference between the quasi Fermi levels at the electrodes, the electric field inverts, leading to the establishment of a drift current. As a result, above the built-in voltage the current no longer shows an exponential voltage behavior, but exhibits a weaker, quadratic voltage dependence in the case of a space-charge-limited device. The built-in voltage is lower than the energy gap of the semiconductor (**Figure 1a**), due

Y. Li, O. Sachnik, B. van der Zee, K. Thakur, C. Ramanan, G.-J. A. H. Wetzelaer, P. W. M. Blom  
Max Planck Institute for Polymer Research  
Ackermannweg 10, 55128 Mainz, Germany  
E-mail: yungui.li@mpip-mainz.mpg.de; wetzelaer@mpip-mainz.mpg.de; blom@mpip-mainz.mpg.de

 The ORCID identification number(s) for the author(s) of this article can be found under <https://doi.org/10.1002/adom.202101149>.

© 2021 The Authors. Advanced Optical Materials published by Wiley-VCH GmbH. This is an open access article under the terms of the Creative Commons Attribution License, which permits use, distribution and reproduction in any medium, provided the original work is properly cited.

DOI: 10.1002/adom.202101149

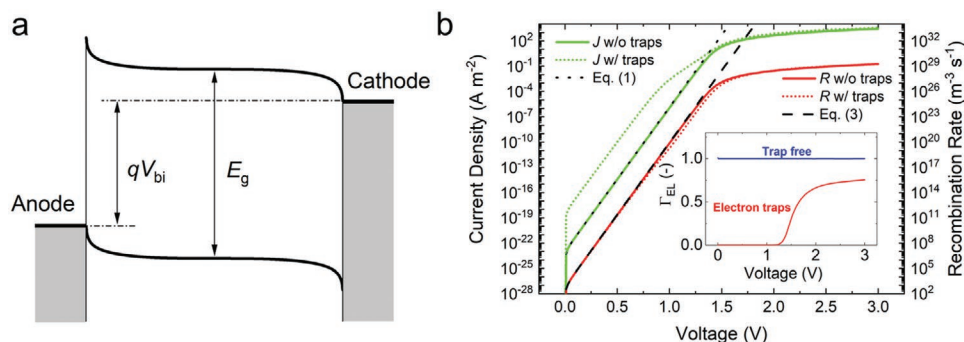


**Figure 1.** Theoretical mechanism of EL at subgap voltages below built-in voltages. a) Energy band diagram of an OLED under quasi-flat-band conditions, at an applied voltage equal to the built-in voltage, indicating that  $qV_{bi} < E_g$  due to band bending near the Ohmic contacts. b) Drift-diffusion simulations<sup>[16]</sup> of the current density and bimolecular recombination rate as a function of voltage for an OLED with  $E_g = 2$  eV without (colored solid lines) and with (colored dotted lines) electron traps at a depth of 0.5 eV at a concentration of  $1 \times 10^{23} \text{ m}^{-3}$ . The black dotted and dashed lines display the current density according to Equation (1) and recombination rate according to Equation (3), respectively. The inset shows  $\Gamma_{EL}$  as a function of voltage.

to charge transfer and associated band bending at the Ohmic contacts, which typically amounts to 0.3–0.4 eV,<sup>[15]</sup> implying that a drift current is even obtained at subgap voltages.

In the ideal case of a semiconductor without traps and Ohmic electron and hole contacts, all the injected carriers recombine and the current is fully dominated by this recombination current, governed by emissive bimolecular recombination, i.e., Langevin recombination. Within the Langevin formalism, the rate-limiting step is the diffusion of electrons and holes until they meet, making Langevin recombination valid for both the diffusion- and drift-dominated current.<sup>[17,18]</sup> As the diffusion current is nonzero for any voltage above 0 V, light emission is also present at any voltage, even close to zero applied voltage, as demonstrated in Figure 1b. Since *all* injected carriers recombine by bimolecular recombination for nondoped OLEDs, the electrical quantum efficiency  $\Gamma_{EL}$  for EL equals unity everywhere down to 0 V, as shown schematically in the inset of Figure 1b.

In a realistic experiment, the semiconductor may likely contain a certain concentration of charge traps. While nonradiative trap-assisted recombination reduces the OLED efficiency, typically with a factor of two in polymer light-emitting diodes (PLEDs),<sup>[19]</sup> EL will still be present down to 0 V, as displayed in Figure 1b by the numerically simulated dotted lines. However, in experiment, since the current in the diffusion regime depends exponentially on voltage, the EL will concomitantly drop sharply below the built-in voltage and, at a certain point, can no longer be detected due to the noise floor of the detector, as shown in Figure S3 in the Supporting Information. In addition, OLEDs typically show a parasitical leakage current at low voltages, partly masking the exponential diffusion-limited current, which will further reduce the EQE at low voltages. The leakage current is, however, not an intrinsic property of the OLED and can be reduced by optimizing fabrication conditions.

The diffusion current and recombination rate at low voltages can also be described analytically. In an OLED at voltages below the built-in voltage, the current density has the same functional dependence as a classical p-n junction, described by the Shockley diode equation

$$J = J_0 \left[ \exp\left(\frac{qV}{\eta kT}\right) - 1 \right] \quad (1)$$

where  $J$  is the current density,  $J_0$  is the reverse-bias saturation current density,  $q$  is the elementary charge,  $V$  is the voltage,  $\eta$  is the ideality factor,  $k$  is the Boltzmann's constant, and  $T$  is the temperature. The ideality factor depends on the recombination mechanism and equals unity for a trap-free semiconductor with only bimolecular recombination, whereas it amounts to 2 in the case of purely trap-assisted recombination. In the case of Ohmic contacts, the current is a recombination current and therefore can be formulated as  $J = qRL$ , with  $R$  the total recombination rate. The Langevin recombination rate is defined as  $R = \gamma(np - n_i^2)$ , with  $\gamma$  the bimolecular recombination coefficient,  $n$  and  $p$  the electron and hole concentration, respectively, and  $n_i$  the intrinsic charge concentration given by  $N_c \exp(-E_g/2kT)$ , with  $N_c$  the density of states. As a result, the reverse-bias saturation current, where  $np \ll n_i^2$ ,<sup>[20]</sup> reads

$$J_0 = q\gamma LN_c^2 \exp\left(-\frac{E_g}{kT}\right) \quad (2)$$

This equation demonstrates that the magnitude of the diffusion current depends on the energy gap of the semiconductor. When substituting Equation (2) into Equation (1) and using  $J = qRL$ , an expression for the recombination rate as a function of voltage is obtained

$$R = \gamma N_c^2 \exp\left(-\frac{E_g}{kT}\right) \left[ \exp\left(\frac{qV}{kT}\right) - 1 \right] \quad (3)$$

which is valid for voltages below the built-in voltage and an ideal semiconductor without traps. In Figure 1b, it is demonstrated that Equation (3) indeed accurately reproduces the numerically simulated recombination rate in the low-voltage regime, while Equation (1) accurately describes the diffusion current. Equation (3) demonstrates that emission at subgap voltages is an intrinsic property of OLEDs. Since the bimolecular recombination coefficient  $\gamma$  is the Langevin coefficient in OLEDs, both the current density and recombination rate will increase for increasing charge-carrier mobilities.<sup>[17]</sup>

For the case of a semiconductor with electron or hole traps, the radiative bimolecular recombination rate will approach Equation (3) at low voltages in the diffusion-dominated regime

and saturate to the same value at 0 V, as shown in Figure 1b. As a result, emission at subgap voltages is not greatly affected by the presence of traps. However, the quantum efficiency for EL is markedly reduced at low voltages due to trapping. This stems from the *increase* of the current at low voltages, as also displayed in Figure 1b. While this appears counterintuitive, the higher ideality factor due to trap-assisted recombination causes the current to decrease less sharply down to 0 V, implying that at a given voltage in the diffusion regime, the current in the presence of trap-assisted recombination is higher. Another way to think of this is that the intrinsic charge concentration in a semiconductor with traps is higher, due to partial filling of the traps in thermal equilibrium. While the total (radiative and nonradiative) recombination rate is stronger in the presence of traps for  $V < V_{bi}$ , the emissive bimolecular recombination rate will remain close to Equation (3), leading to the observation of EL at subgap voltages even in the presence of traps. It should be noted that in the presence of both electron and hole traps, the drift current reduces due to decreased charge transport (cf. decreased mobilities), which in turn reduces EL in the drift regime, complicating experimental detection.

To confirm the universal presence of EL at subgap voltage experimentally, we have fabricated simple OLEDs consisting of a single semiconductor layer sandwiched between two charge-injecting electrodes. For semiconductors, fluorescent conjugated polymers or small-molecular emitters that exhibit thermally activated delayed fluorescence (TADF) were chosen. We have recently demonstrated an energy window for trap-free transport in organic semiconductors. Semiconductors with an electron affinity larger than 3.5 eV exhibit trap-free electron transport, whereas materials with an ionization energy smaller than 6.0 eV exhibit trap-free hole transport.<sup>[21]</sup> The energy levels of the TADF emitter CzDBA (9,10-bis(4-(9*H*-carbazol-9-yl)-2,6-dimethylphenyl)-9,10-diboraanthracene) fit almost exactly in this window, such that both the electron and hole transport are nearly trap free.<sup>[22,23]</sup> The EQE of single-layer undoped CzDBA OLEDs reaches values of up to 20%.<sup>[23,24]</sup> The chemical structure of CzDBA is shown in Figure 2a. Furthermore, a single-layer OLED based on CzDBA has a nearly 100% internal quantum efficiency, such that this is an excellent model system that approaches the ideal case described above.<sup>[24]</sup> Furthermore, TADF emitters like CzDBA have only a small splitting of up to several tens of meV between the singlet and triplet excited

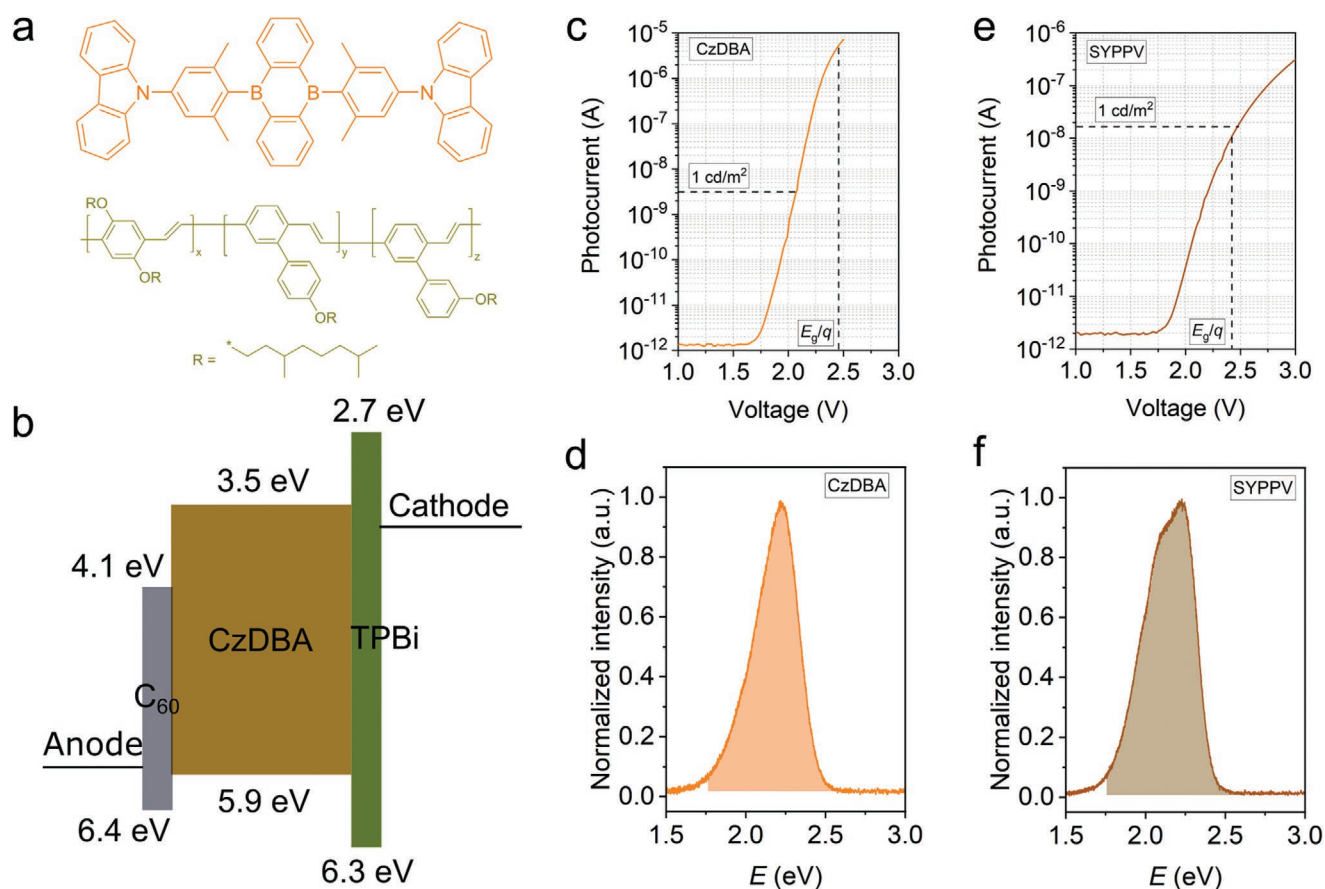


**Figure 2.** EL at voltages below the energy gap. The chemical structure of organic emitters CzDBA and SY-PPV are shown in (a), in which CzDBA is shown on the top and SY-PPV on the bottom. b) Device structure for CzDBA devices, comprising 4 nm C<sub>60</sub> and TPBi (2,2',2''-(1,3,5-benzinetriyl)-tris(1-phenyl-1*H*-benzimidazole)) tunneling interlayers for efficient charge injection.<sup>[21,23]</sup> Photocurrent detected by a photodiode as a function of driving voltages for c) CzDBA and e) SY-PPV OLEDs. The horizontal dashed line indicates a luminance of 1 cd m<sup>-2</sup>, while the vertical dashed line represents the voltage corresponding to the energy gap ( $E_g/q$ ). The shaded area of the EL spectra in d) CzDBA at 2.4 V, and f) SY-PPV indicates emitted photons with higher energy than  $qV_{th}$  for each device.

state, which enables reverse intersystem crossing from the triplet excitons to singlet excitons by means of thermal energy, resulting in delayed fluorescence. In conventional fluorescent emitters like conjugated polymers, the splitting between the singlet and triplet state is typically about 0.7 eV, and for some emitters the triplet state has only half the energy of the singlet state.<sup>[25,26]</sup> In previous reports, EL at subgap voltages was observed, assuming that a large singlet-triplet splitting was responsible for the low-voltage operation, based on the premise that low-energy triplet excitons could be formed by direct charge injection at low voltage, followed by triplet fusion resulting in emissive singlet states.<sup>[1,4]</sup>

As demonstrated in Figure 2c,d, EL at subgap voltage is clearly observed for CzDBA, of which the triplet excited state is only 33 meV below the singlet excited state. The threshold voltage ( $V_{th}$ ) to observe EL, which depends on the sensitivity of the photodetector, equals  $\approx 1.7$  V, which is much lower than  $E_g/q$ , with  $E_g$  of 2.48 eV for CzDBA.<sup>[22]</sup> This unambiguously shows that a large singlet-triplet splitting is not required for observing EL at voltages below the energy gap, and that TTA can be ruled out as the responsible mechanism. Even if direct injection into the triplet state were possible, the voltage required would be negligibly less than needed for singlet-state excitation. Rather, the light emission at subgap voltages as observed here is a general feature of OLEDs (Figure S1, Supporting Information), with EL spectra from UV to blue and red region, based on emitters with either conventional fluorescent or TADF emitters. The universal EL at subgap voltages from OLEDs originates from the diffusion of charge carriers as described above.

To measure the EL spectrum at low voltages with low intensity, the EL spectra of the CzDBA device with high EQE at low voltages are measured with a streak camera. The EL spectra from 1.9 to 2.3 V are shown as Figure S4 in the Supporting Information. It shows that the photon energy of the EL spectra at subgap voltages has much higher energy than  $qV$ . It also demonstrates that the detected EL is indeed produced by singlet emission by CzDBA. Other sources of emission, such as exciplex emission from the  $C_{60}$ /CzDBA interface can be excluded, as  $C_{60}$  is not used as an electron transport layer, but as an interlayer to enhance hole injection (Figure 2b and Figure S5, Supporting Information), such that electrons are not injected into  $C_{60}$ , and holes tunnel through it. Furthermore, it has been demonstrated that the charge recombination does not take place at this interface, with the recombination zone shifting even further away at low voltages.<sup>[23]</sup> In addition, EL at subgap voltages is also detected for polymer OLEDs in which  $C_{60}$  is not present (vide infra).

It should be noted that TTA-mediated emission may still play a certain role in carefully constructed heterojunction devices via the formation of an interfacial charge-transfer state, although such mechanism has not been unambiguously demonstrated. In general, to achieve a significant fraction of TTA-induced singlet excitons, a high density of triplet excitons is required. However, the exciton density at voltages below  $V_{bi}$  in a typical OLED is low, minimizing the encounter probability for triplet excitons.

As presented in Figure 2 and Figure S1 in the Supporting Information, emission at subgap voltages is also observed for OLEDs based on the fluorescent conjugated polymers super

yellow poly(*p*-phenylene vinylene) (SY-PPV, Figure 2a) and poly[2-methoxy-5-(2-ethylhexyloxy)-1,4-phenylenevinylene] (MEH-PPV). As shown in Figure S2 in the Supporting Information, the EQE is  $\approx 5\%$  for SY-PPV OLEDs, and 2% for MEH-PPV OLEDs. We note that for these conventional fluorescent polymers with 25% generation of singlet excitons and 20% out-coupling efficiency, an EQE of 5% is the theoretical maximum, demonstrating that also these PLEDs are relatively efficient. In contrast to the TADF emitter CzDBA, conjugated polymers typically contain a substantial concentration of electron traps, in the order of  $10^{23} \text{ m}^{-3}$ .<sup>[27]</sup> Therefore, nonradiative trap-assisted recombination in conjugated polymers is the dominant recombination mechanism at low voltages. Nevertheless, as shown in Figure 2e,f, EL is still observed at voltages below the energy gap. Since nonradiative trap-assisted and radiative bimolecular recombination are competing processes, the efficiency of EL is lower at low voltages. In the diffusion regime, the ideality factor of the current will be approximately equal to 2 in accordance with the dominant contribution stemming from trap-assisted recombination, while the luminance has an ideality factor close to 1, consistent with radiative bimolecular recombination, as previously demonstrated experimentally.<sup>[28,29]</sup> As a result, the diffusion current depends less strongly on voltage than the luminance, resulting in lower quantum efficiencies at low voltages in the presence of nonradiative trap-assisted recombination, schematically indicated in the inset of Figure 1b.

Lastly, it has also been proposed that the use of a high-work function cathode could promote direct injection into the low-energy triplet state of an emitter, leading to low “turn-on” voltages.<sup>[7]</sup> The observance of low-voltage emission in this case may alternatively be understood from a device physics point of view without the need of incorporating triplet states. By using a high-work function cathode, the built-in voltage due to the work-function difference between anode and cathode is reduced. As a result, a smaller voltage is required to establish a (mainly unipolar) drift current. In turn, EL may also be observed at low voltages given a sufficiently sensitive photodetector. Here, EL originates from bimolecular recombination of majority carriers (holes) with thermally excited electrons in the conduction band near the cathode, its concentration being determined by the Fermi level of the cathode. However, EL will be inefficient because of most holes disappearing via surface recombination at the cathode.

Even in case of an electron-injection barrier  $\phi_b$ , the bimolecular recombination rate below the built-in voltage will still be given by Equation (3). The hole density near the cathode in such a hole-dominated device is given by

$$p = N_c \exp\left(\frac{\phi_b - E_g}{kT}\right) \exp\left(\frac{qV}{kT}\right) \quad (4)$$

for  $V < V_{bi}$ . Holes will recombine with electrons near the cathode interface, where the electron density is given by  $n = N_c \exp(-\phi_b/kT)$ , without considering the image force and field-dependent barrier lowering effect. Calculating the bimolecular recombination rate from the product  $np$  according to  $R = \gamma(np - n_i^2)$  results in the same expression as given by Equation (3), as can be seen in Figure 3a from the unchanged exponential part of the  $R$ - $V$  characteristics when modifying the

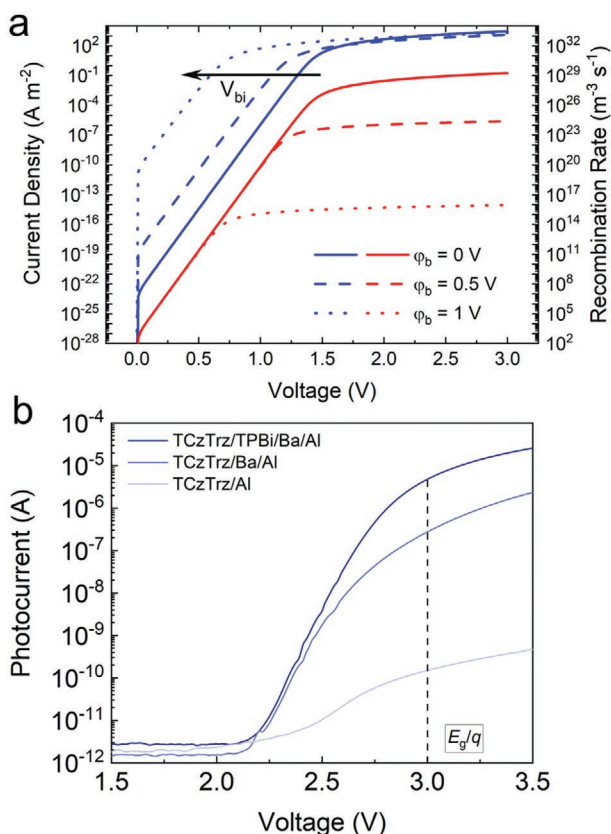


**Figure 3.** Impact of injection barrier on the voltage dependence of the EL intensity. a) Simulated current density and bimolecular recombination rate as a function of voltage for different values of the cathode barrier  $\phi_b$ . Increasing  $\phi_b$  results in a reduced built-in voltage, shifting the  $J$ - $V$  characteristics along the voltage axis. The recombination rate remains the same for  $V < V_{bi}$ , while it reduces strongly for  $V > V_{bi}$ . b) Observation of EL at subgap voltage from OLEDs with different injection barriers. Lower EL intensity is detected for OLEDs with a higher injection barrier.

cathode injection barrier. However, because of the higher current density at low voltages due to the lower built-in voltage, the EL efficiency will be greatly reduced, despite the same bimolecular recombination rate for  $V < V_{bi}$ .

Experimentally, we employed the blue-emitting TADF material TCzTrz (9,9'-(5-(4,6-diphenyl-1,3,5-triazin-2-yl))-1,3-phenylene)bis(9*H*-carbazole) with the lowest unoccupied molecular orbital level located at 2.86 eV.<sup>[30,31]</sup> In single-layer OLEDs, a 4 nm TPBi interlayer, as used in CzDBA single-layer OLEDs,<sup>[23]</sup> was found to enhance electron injection. To vary the injection barrier, Ba/Al and Al cathodes are used without TPBi tunneling interlayer. As can be seen in Figure 3b and Figure S2 in the Supporting Information, even for the large injection barrier at the Al cathode, EL is observed at subgap voltages. The combination of a large bandgap and large electron injection barrier strongly reduces the number of free carriers in the OLED. Since Auger recombination is a three-particle process that is only relevant at high carrier density this can also be excluded as possible origin of EL at subgap voltage. We note that in experiment, a large contact barrier will complicate the detection of EL at subgap voltages, unless a sufficiently sensitive photodetector is used. Since in experiments OLEDs frequently exhibit injection barriers,

barriers at heterojunctions, low charge-carrier mobilities, and/or charge traps, together with relatively insensitive photodetectors, EL at subgap voltages is only rarely observed, although being a universal phenomenon.

### 3. Conclusion

In conclusion, we have demonstrated that EL at applied voltages below the energy gap of the emitter is a universal feature in OLEDs, originating from the recombination of diffused charge carriers below the built-in voltage. An expression for the recombination rate below the built-in voltage is formulated, rationalizing the experimentally observed luminance-voltage behavior at low voltages. Theoretically, EL occurs down to zero applied voltage, but is usually not detected in experiment due to the sensitivity limits of the photodetector. By using OLEDs based on TADF emitters, we rule out TTA as an origin for EL at low voltage, since in such emitters the triplet and singlet excited states are nearly identical. To observe EL at subgap voltages, the emitter is ideally free of charge traps, has a high charge-carrier mobility and low injection or heterojunction barriers.

The implication of these results is that it would be theoretically possible to achieve electrical-to-optical power-conversion efficiencies above unity in OLEDs, in case the applied voltage is lower than  $E_g/q$ . In an ideal OLED, the internal quantum efficiency equals unity in this voltage regime in case of an efficient emitter with 100% photoluminescence quantum yield and without nonradiative trap-assisted recombination, while the electrical energy per charge is lower than the optical output energy per photon. The extra energy required to fulfil the law of energy conservation stems from the thermal energy present at nonzero temperatures. However, it should be noted that power-conversion efficiencies above unity would be difficult to achieve in terms of external efficiencies, mainly due to high light-out-coupling losses, which reduce the EQE significantly.

### Supporting Information

Supporting Information is available from the Wiley Online Library or from the author.

### Acknowledgements

The authors thank Christian Bauer and Frank Keller for technical support. Open access funding enabled and organized by Projekt DEAL.

### Conflict of Interest

The authors declare no conflict of interest.

### Data Availability Statement

The data that support the findings of this study are available from the corresponding author upon reasonable request.

## Keywords

built-in voltage, conjugated polymers, organic light-emitting diodes, subgap voltage electroluminescence, thermally activated delayed fluorescence

Received: June 8, 2021

Revised: July 10, 2021

Published online:

- 
- [1] C. Xiang, C. Peng, Y. Chen, F. So, *Small* **2015**, *11*, 5439.
- [2] L. Qian, Y. Zheng, K. R. Choudhury, D. Bera, F. So, J. Xue, P. H. Holloway, *Nano Today* **2010**, *5*, 384.
- [3] B. Y. Lin, C. J. Easley, C. H. Chen, P. C. Tseng, M. Z. Lee, P. H. Sher, J. K. Wang, T. L. Chiu, C. F. Lin, C. J. Bardeen, J. H. Lee, *ACS Appl. Mater. Interfaces* **2017**, *9*, 10963.
- [4] A. K. Pandey, J. M. Nunzi, *Adv. Mater.* **2007**, *19*, 3613.
- [5] A. K. Pandey, J.-M. Nunzi, *Appl. Phys. Lett.* **2007**, *90*, 263508.
- [6] X. Qiao, D. Ma, *Nat. Commun.* **2019**, *10*, 4683.
- [7] A. Salehi, C. Dong, D.-H. Shin, L. Zhu, C. Papa, A. Thy Bui, F. N. Castellano, F. So, *Nat. Commun.* **2019**, *10*, 2305.
- [8] Q. Chen, W. Jia, L. Chen, D. Yuan, Y. Zou, Z. Xiong, *Sci. Rep.* **2016**, *6*, 25331.
- [9] S. Engmann, A. J. Barito, E. G. Bittle, N. C. Giebink, L. J. Richter, D. J. Gundlach, *Nat. Commun.* **2019**, *10*, 227.
- [10] S. Engmann, A. J. Barito, E. G. Bittle, N. C. Giebink, L. J. Richter, D. J. Gundlach, *Nat. Commun.* **2019**, *10*, 4684.
- [11] G. C. Dousmanis, C. W. Mueller, H. Nelson, K. G. Petzinger, *Phys. Rev.* **1964**, *133*, A316.
- [12] P. Santhanam, D. J. Gray, R. J. Ram, *Phys. Rev. Lett.* **2012**, *108*, 097403.
- [13] A. G. Mal'shukov, K. A. Chao, *Phys. Rev. Lett.* **2001**, *86*, 5570.
- [14] M. I. Nathan, G. Burns, S. E. Blum, J. C. Marinace, *Phys. Rev.* **1963**, *132*, 1482.
- [15] P. de Bruyn, A. H. P. van Rest, G. A. H. Wetzelaer, D. M. de Leeuw, P. W. M. Blom, *Phys. Rev. Lett.* **2013**, *111*, 186801.
- [16] L. J. A. Koster, E. C. P. Smits, V. D. Mihailetschi, P. W. M. Blom, *Phys. Rev. B: Condens. Matter Mater. Phys.* **2005**, *72*, 085205.
- [17] M. Kuik, G.-J. A. H. Wetzelaer, H. T. Nicolai, N. I. Craciun, D. M. De Leeuw, P. W. M. Blom, *Adv. Mater.* **2014**, *26*, 512.
- [18] Q. Niu, N. I. Crăciun, G.-J. A. H. Wetzelaer, P. W. M. Blom, *Phys. Rev. Lett.* **2018**, *120*, 116602.
- [19] D. Abbaszadeh, A. Kunz, G. A. H. Wetzelaer, J. J. Michels, N. I. Crăciun, K. Koynov, I. Lieberwirth, P. W. M. Blom, *Nat. Mater.* **2016**, *15*, 628.
- [20] S. M. Sze, K. K. Ng, *Physics of Semiconductor Devices*, 3rd ed., John Wiley & Sons, Inc., New York **2007**.
- [21] N. B. Kotadiya, H. Lu, A. Mondal, Y. Ie, D. Andrienko, P. W. M. Blom, G. J. A. H. Wetzelaer, *Nat. Mater.* **2018**, *17*, 329.
- [22] T.-L. Wu, M.-J. Huang, C.-C. Lin, P.-Y. Huang, T.-Y. Chou, R.-W. Chen-Cheng, H.-W. Lin, R.-S. Liu, C.-H. Cheng, *Nat. Photonics* **2018**, *12*, 235.
- [23] N. B. Kotadiya, P. W. M. Blom, G.-J. A. H. Wetzelaer, *Nat. Photonics* **2019**, *13*, 765.
- [24] Y. Li, N. B. Kotadiya, B. Zee, P. W. M. Blom, G. A. H. Wetzelaer, *Adv. Opt. Mater.* **2021**, *9*, 2001812.
- [25] A. Köhler, J. S. Wilson, R. H. Friend, M. K. Al-Suti, M. S. Khan, A. Gerhard, H. Bässler, *J. Chem. Phys.* **2002**, *116*, 9457.
- [26] A. Köhler, D. Beljonne, *Adv. Funct. Mater.* **2004**, *14*, 11.
- [27] N. B. Kotadiya, A. Mondal, P. W. M. Blom, D. Andrienko, G. J. A. H. Wetzelaer, *Nat. Mater.* **2019**, *18*, 1182.
- [28] G. A. H. Wetzelaer, L. J. A. Koster, P. W. M. Blom, *Phys. Rev. Lett.* **2011**, *107*, 066605.
- [29] G.-J. A. H. Wetzelaer, P. W. M. Blom, *NPG Asia Mater.* **2014**, *6*, e110.
- [30] M. Kim, S. K. Jeon, S. H. Hwang, J. Y. Lee, *Adv. Mater.* **2015**, *27*, 2515.
- [31] S. K. Jeon, K. S. Yook, J. Y. Lee, *Nanotechnology* **2016**, *27*, 224001.